Supporting Information

Mechanistic Insights into Formation of CO and C2 Products in Electrochemical CO_2 Reduction – the Role of the ECE Mechanism

Rileigh Casebolt DiDomenico, Kelsey Levine, Laila Reimanis, Hector Abruña, and Tobias Hanrath

1. **Comparison of linear sweep voltammogram and potentiostatic measurements.**
   Figure S1 compares the linear sweep voltammogram (LSV) from -0.3V to -2.0V vs Ag/AgCl at 10 mV/s in 1M KCl on polycrystalline copper with constant potential CO_2 reduction at potentials from -1.4V to -1.8V. The total measured current agrees well with the LSV trace. As seen in 0.1M $KHCO_3$ by Kuhl et al., we also find that the LSV can be reconstructed from chronoamperometry experiments, a technique known as sampled-current voltammetry.[1, 2]

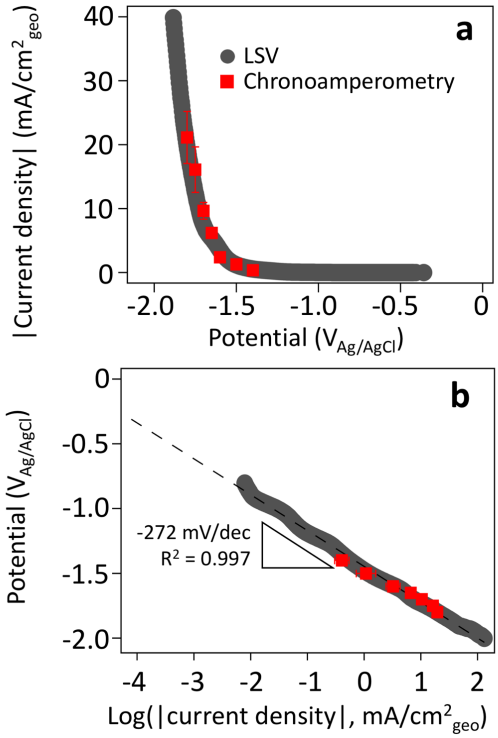

Figure S1. (a) LSV (current density versus potential) when scanning at 10 mV/s (grey circles) and total measured current density (red squares) from chronoamperometry after 10 minutes (error bars are mean ± one standard deviation from n = 3 separate replicates). (b) Tafel plot for LSV and chronoamperometry data, where the slope of the line is equal to the overpotential required to achieve a decade increase in current density. Both LSV and chronoamperometry data are the total current density from HER and CO2R together. Good Tafel fit indicates highly irreversible electrochemical reaction kinetics.

2. Tafel plots for C_2H_4, CH_4, HCOOH, and CO

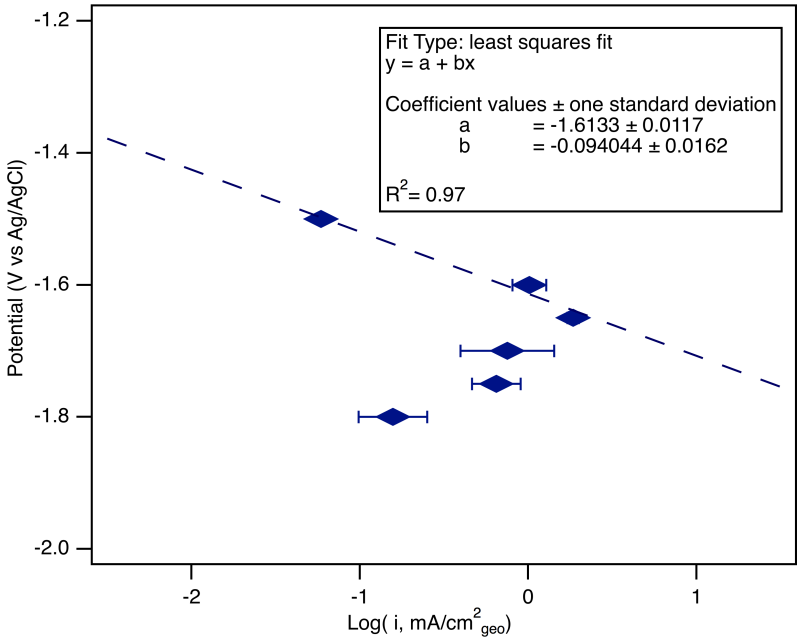

Figure S2. Tafel plot for C_2H_4 corresponding to Figure 1c in the main text. Fit was calculated for first three points on rising edge of volcano (-1.4V to -1.6V) to determine a slope of about 94 mV/dec.

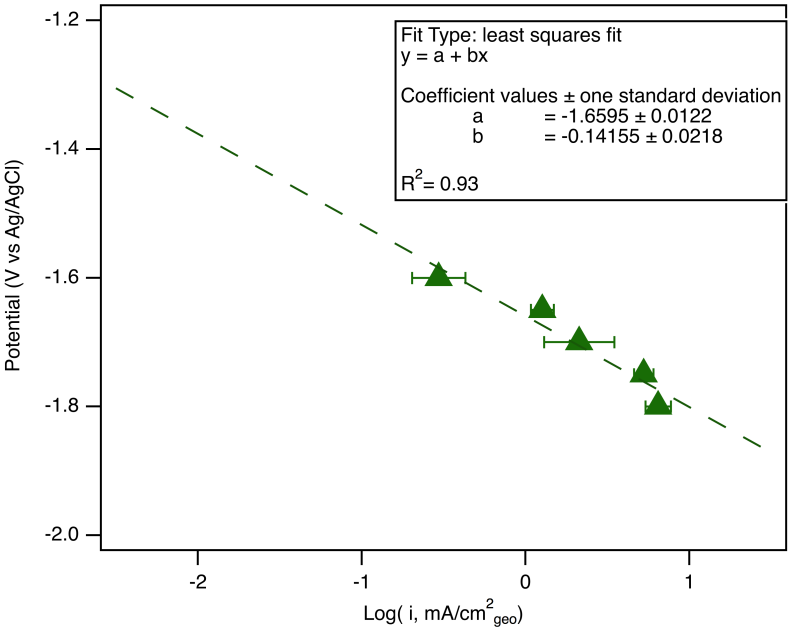

Figure S3. Tafel plot for CH_4 corresponding to Figure 1c in the main text. Slope was found to be about 142 mV/dec.

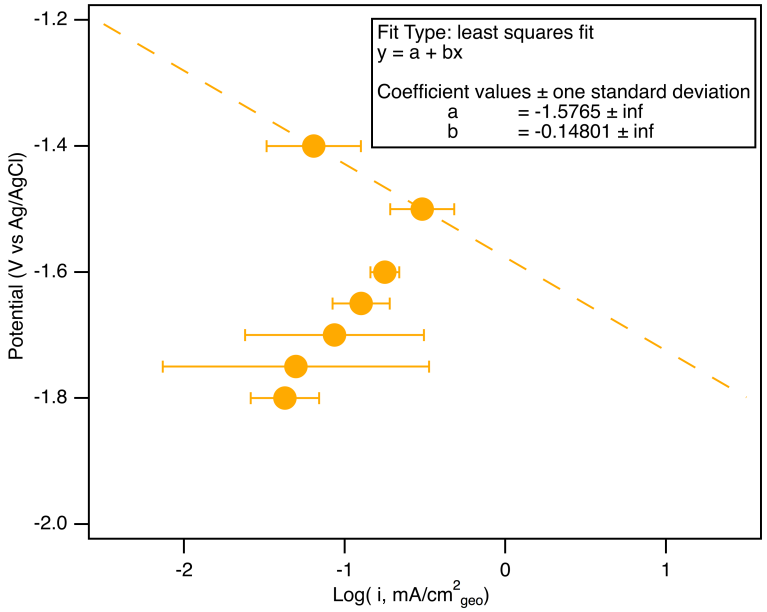

Figure S4. Tafel plot for CO corresponding to Figure 1c in the main text. Fit was calculated for first two points on rising edge of volcano (-1.4V to -1.5V) before activity trend reversed to determine a slope of about 148 mV/dec. This is an estimation based on only two points, so more experiments in the active region would need to be conducted before reporting an official Tafel slope value, however this is on par with the 118 mV/dec slope expected for the process.[3]

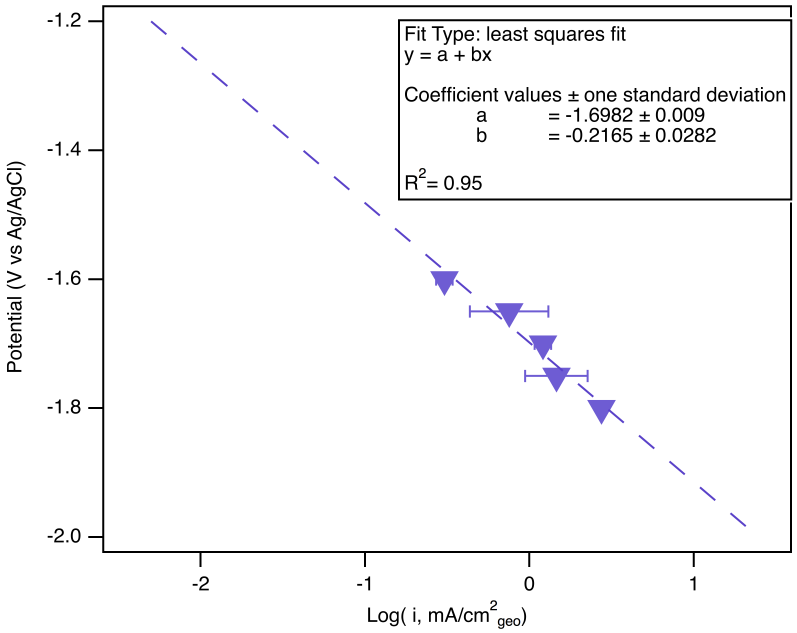

Figure S5. Tafel plot for HCOOH corresponding to Figure 1c in the main text. Slope was found to be about 217 mV/dec.

3. Electrode surface roughness estimate from double layer capacitance

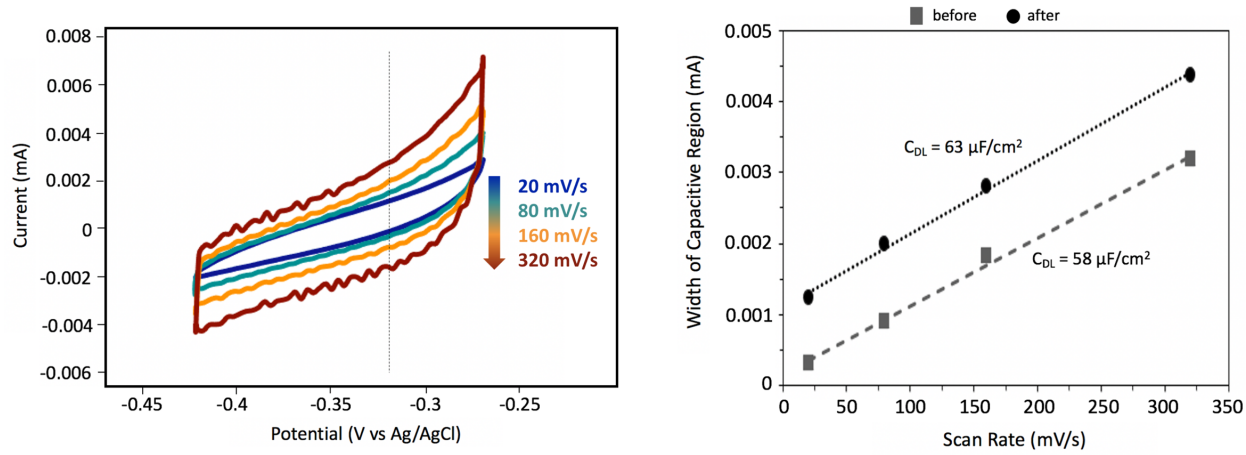

Figure S6. (left) CV scans from -0.27V to -0.42V vs Ag/AgCl at increasing scan rates to estimate double layer capacitance of polycrystalline copper foil electrode before and after electrolysis. Vertical dotted line at -0.32V indicates the potential at which capacitance measurements were made. (right) Width of the non-Faradaic capacitive region at -0.32V vs Ag/AgCl as a function of scan rate where the slope is equivalent to capacitance. The roughness factor calculated as $C_{DL,after}$ divided by $C_{DL,before}$ is about 1.08 indicating negligible roughening takes place over the course of 1 hour electrolysis at -1.6V. This is representative of the calculated roughness factors after all of the experiments at varying potentials. These capacitances are comparable to the 67 µF/cm^2 identified by Zhong et al. for their copper foil.[4]

4. Detailed description of the Cottrell fitting algorithm

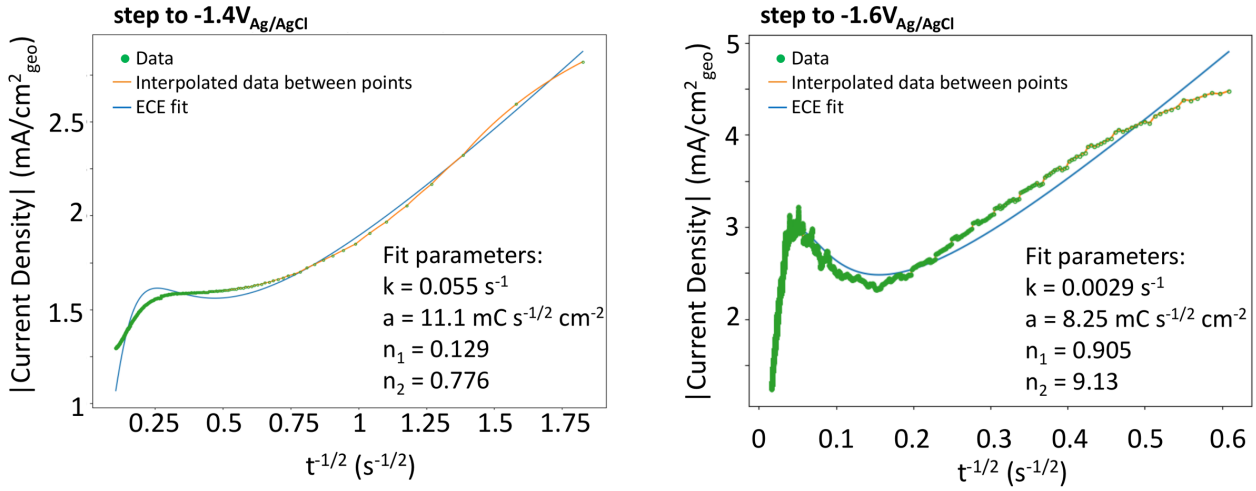

Figure S7. (left) Cottrell plot (I vs $t^{-1/2}$) for CO_2-saturated 1M KCl when potential is stepped to -1.4V vs Ag/AgCl with ECE fit corresponding to Figure 3b in the main text. Optimized parameters found by Python scipy.optimize.curve_fit function listed on plot. Data was fit to ECE equation presented by Murray[5] and listed as Equation 4 in main text. $R^2 = 0.99$. (right) Cottrell plot (I vs $t^{-1/2}$) for CO_2-saturated 1M KCl when potential is stepped to -1.6V vs Ag/AgCl with ECE fit corresponding to Figure 4b in main text. Optimized parameters found by Python scipy.optimize.curve_fit function listed on plot. $R^2 = 0.96$ when fit from $0 < t^{-1/2} < 0.6$. At $t^{-1/2} > 0.6$, data bends off Cottrell line due to pre-kinetics.

We calculated the value of *a* separately to compare our parameter estimation to that of the scipy program.

$$a = FC_0^b\sqrt{\frac{D}{\pi}}$$

$$= 96{,}485\ \frac{C}{mol} * 3.4x10^{-5}\frac{mol}{cm^3} * \sqrt{\frac{40x10^{-6}\frac{cm^2}{s}}{\pi}} = 0.0117\frac{C}{s^{\frac{1}{2}}cm^2} = 11.7\frac{mC}{s^{\frac{1}{2}}cm^2}$$

Where *F* is Faraday's constant, C_0^b is the initial CO_2 concentration which is about 0.034 mol/L,[6] and *D* is the diffusion coefficient of CO_2 in 1M KCl which is about $40x10^{-6}$ cm^2/s.[7]

This aligns well with the value of *a* identified by the scipy.optimize.curve_fit function.

We also set the value of n_1 to show the insensitivity of the n_2/n_1 ratio and *k* value.

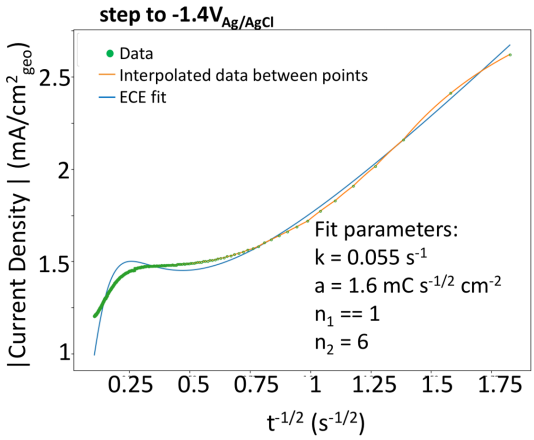

Figure S8. Cottrell plot (I vs $t^{-1/2}$) for CO_2-saturated 1M KCl when potential is stepped to -1.4V vs Ag/AgCl with ECE fit when n_1 is set to 1.

Notice that the optimized parameters found by Python scipy.optimize.curve_fit function are essentially unchanged from Figure S8: *k* is the same and the ratio of n_2 to n_1 is still 6. $R^2 = 0.99$.

5. Possible reaction pathways from CO_2 to CO

A recent study by Deng et al., used pH and kinetic isotope experiments to determine the rate determining step (RDS) reaction order for H^+ and H_2O should be 0.[8] Their analysis concluded that CO_2 adsorption in pathway 1 is the only possible RDS (bolded steps). The ECE analysis described in our study corroborates this conclusion and confirms that alternate pathways (shaded in grey), which don't include an interposed chemical step, can be ruled out.

Table S1. Possible reaction pathways to form CO from CO_2 using steps presented by Deng et al where proton donor can be H^+ or H_2O depending on the electrolyte environment.[8]

Pathway	Possible Reaction Steps	Step Type	Reaction Mechanism
1 Proton donor: H^+	**$CO_2 + * + e^- \rightarrow *CO_2^-$** $*CO_2^- + H^+ \rightarrow *COOH$ $*COOH + e^- \rightarrow *COOH^-$ $*COOH^- + H^+ \rightarrow *CO + H_2O$ $*CO \rightarrow CO + *$	ET PT ET PT D	ECECD
2 Proton donor: H^+	$CO_2 + * + e^- + H^+ \rightarrow *COOH$ $*COOH + e^- \rightarrow *COOH^-$ $*COOH^- + H^+ \rightarrow *CO + H_2O$ $*CO \rightarrow CO + *$	PCET ET PT D	EECD
3 Proton donor: H^+	$CO_2 + * + e^- + H^+ \rightarrow *COOH$ $*COOH + e^- + H^+ \rightarrow *CO + H_2O$ $*CO \rightarrow CO + *$	PCET PCET D	EED

Using a simple chronoamperometric study, we were able to identify CO_2 through $*CO_2^-$ to CO through decoupled electron and proton transfer steps (Table S1, Pathway 1) as the most likely CO formation mechanism, narrowing in on the same pathways as a recent study using a completely different experimental technique.[8]

6. References

1. Kuhl, K. P., Cave, E. R., Abram, D. N., Jaramillo, T. F. (2012). New insights into the electrochemical reduction of carbon dioxide on metallic copper surfaces. Energy Environ. Sci. 5, 7050-7059. https://doi.org/10.1039/C2EE21234J.
2. Bard, A., Faulkner, L. (2001). Electrochemical Methods: Fundamentals and Applications 2nd ed.; (John Wiley & Sons, Inc.).
3. Li, J., Chang, X., Zhang, H., Malkani, A. S., Cheng, M.-j., Xu, B., Lu, Q. (2021). Electrokinetic and in situ spectroscopic investigations of CO electrochemical reduction on copper. Nat. Commun. 12, 1-11. https://doi.org/10.1038/s41467-022-28436-z.
4. Zhong, D., Zhao, Z. J., Zhao, Q., Cheng, D., Liu, B., Zhang, G., Deng, W., Dong, H., Zhang, L., Li, J. (2021). Coupling of Cu(100) and (110) facets promotes carbon dioxide conversion to

hydrocarbons and alcohols. Angew. Chem., Int. Ed. 60, 4879-4885. https://doi.org/10.1002/anie.202015159.
5. Murray, R. (1971). Chronoamperometry, Chronocoulometry, and Chronopotentiometry In Techniques of Chemistry, Weissberger, A.,Rossiter, B., Eds. John Wiiley & Sons, Inc.: pp 591-644.
6. Gupta, N., Gattrell, M., MacDougall, B. (2006). Calculation for the cathode surface concentrations in the electrochemical reduction of CO2 in KHCO3 solutions. J. Appl. Electrochem. 36, 161-172. https://doi.org/10.1007/s10800-005-9058-y.
7. Casebolt, R., Kimura, K. W., Levine, K., Cimada DaSilva, J. A., Kim, J., Dunbar, T. A., Suntivich, J., Hanrath, T. (2021). Effect of electrolyte composition and concentration on pulsed potential electrochemical CO2 reduction. ChemElectroChem. 8, 681-688. https://doi.org/10.1002/celc.202001445.
8. Deng, W., Zhang, P., Seger, B., Gong, J. (2022). Unraveling the rate-limiting step of two-electron transfer electrochemical reduction of carbon dioxide. Nat. Commun. 13, 1-9. https://doi.org/10.1038/s41467-022-28436-z.